

# Antisense PNA Accumulates in *Escherichia coli* and Mediates a Long Post-antibiotic Effect

Abbas Nikravesh<sup>1,2</sup>, Rikard Dryselius<sup>1,3</sup>, Omid R Faridani<sup>1</sup>, Shan Goh<sup>1</sup>, Majid Sadeghizadeh<sup>2</sup>, Mehrdad Behmanesh<sup>2</sup>, Anita Ganyu<sup>1</sup>, Erik Jan Klok<sup>4</sup>, Rula Zain<sup>5</sup> and Liam Good<sup>1</sup>

<sup>1</sup>Department of Cell and Molecular Biology, Karolinska Institutet, Stockholm, Sweden; <sup>2</sup>Department of Genetics, Faculty of Basic Sciences, Tarbiat Modares University, Tehran, Iran; <sup>3</sup>Department of Bacterial Infections, Research Institute for Microbial Diseases, Osaka University, Osaka, Japan; <sup>4</sup>KREATECH Biotechnology B.V., Amsterdam, The Netherlands; <sup>5</sup>Department of Molecular Biology and Functional Genomics, Stockholm University, Stockholm, Sweden

Antisense agents that target growth-essential genes display surprisingly potent bactericidal properties. In particular, peptide nucleic acid (PNA) and phosphorodiamidate morpholino oligomers linked to cationic carrier peptides are effective in time kill assays and as inhibitors of bacterial peritonitis in mice. It is unclear how these relatively large antimicrobials overcome stringent bacterial barriers and mediate killing. Here we determined the transit kinetics of peptide–PNAs and observed an accumulation of cell-associated PNA in *Escherichia coli* and slow efflux. An inhibitor of drug efflux pumps did not alter peptide–PNA potency, indicating a lack of active efflux from cells. Consistent with cell retention, the post-antibiotic effect (PAE) of the anti-acyl carrier protein (*acpP*) peptide–PNA was greater than 11 hours. Bacterial cell accumulation and a long PAE are properties of significant interest for antimicrobial development.

Received 11 February 2007; accepted 20 April 2007; published online 29 May 2007; doi:10.1038/sj.mt.6300209

## INTRODUCTION

Antibiotic resistance is an important medical problem that threatens to reverse or diminish the “antibiotic miracle”. Moreover, the development of new drugs using conventional strategies is unlikely to keep pace with acquired resistance. Only two new classes of antimicrobial agents have been introduced into the clinic in the past 35 years. Therefore, new types of antimicrobials, particularly to treat persistent and multi-drug resistant infections,<sup>1</sup> are urgently needed.

To help provide new types of antimicrobial agents and tools for microbial genetics, antisense technologies have been developed for bacterial applications. Antisense agents are attractive for research and therapeutic development because they offer the possibility of using simple design rules to inhibit any gene. Bacteria themselves use natural antisense mechanisms<sup>2</sup> and may be uniquely amenable to antisense control. For example, bacteria have relatively small genomes and lack organelles, features that naturally increase the chance of target binding and hence of

gene-specific effects. However, bacteria typically exclude foreign molecules with stringent cell barriers and efflux pumps. Fortunately, new nucleic acid analogues and mimics—such as peptide nucleic acid (PNA) and phosphorodiamidate morpholino oligomers—have been developed.<sup>3,4</sup> Although such oligomers are larger than conventional antibiotics, their uncharged backbones appear to enable delivery across negatively charged bacterial cell barriers, and positively charged amino acids can be added to provide cationic regions within the molecule. These delivery advantages have also been exploited in diagnostics applications to provide improved antisense probes for *in situ* staining of microbes.<sup>5,6</sup>

PNA uptake and antisense effects can be improved using short (*e.g.*, 10–12-mer) PNAs and attachment to cationic carrier peptides that permeabilize bacterial membranes (*e.g.*, KFFKFFKFFK).<sup>7,8</sup> Indeed, a peptide–PNA directed against the messenger RNA (mRNA) encoding the essential acyl carrier protein (*acpP*), which is central to fatty acid biosynthesis, shows bactericidal properties in *Escherichia coli* at nanomolar to low micromolar concentrations.<sup>7,9</sup> Certain peptide–PNA and peptide–phosphorodiamidate morpholino oligomers targeted against growth-essential genes are more bactericidal *in vitro* and *in vivo* relative to molar or mass equivalent doses of ampicillin and rifampicin, and they act with sequence and gene selectivity.<sup>7,10–13</sup> Also, a variety of target genes and possibly a range of species can be targeted.<sup>14–18</sup> One possible explanation for this potent killing activity is that antisense molecules accumulate in bacteria, as reported for certain antibiotics, including rifampicin.<sup>19</sup>

Here we studied the antibacterial effects of antisense peptide–PNAs to understand how these relatively large molecules are able to mediate potent cell killing. Cell morphology, cell transit kinetics, and post-antibiotic effects (PAEs) were assessed using two antisense peptide–PNAs that target the non-essential *lacZ* and essential *acpP* genes at the mRNA level. Conventional antibiotics were included for comparison. The results indicate an accumulation of cell-associated PNA and slow efflux. Consistent with the cellular transit data, an anti-*acpP* peptide–PNA showed a strong PAE (>11 hours). Thus, although the delivery of antisense agents into bacteria is a significant challenge, once delivered the molecule is retained, and this appears to contribute to the bactericidal

**Correspondence:** Liam Good, Department of Cell and Molecular Biology (CMB), Karolinska Institutet, Berzelius väg 35, 171 77 Stockholm, Sweden. E-mail: liam.good@ki.se

activity. Such accumulation and retention properties are interesting with respect to the potential of antisense agents as drugs to treat infections, particularly infections involving persistent or drug resistant bacteria.

## RESULTS

### Anti-*acpP* peptide-PNA has comparatively potent bactericidal activity

Antisense antibacterials show potent bactericidal effects relative to ampicillin in *in vivo* infection models and also *in vitro*.<sup>9,11,13</sup> Here we aimed to extend this comparison to additional conventional antibiotics and examine the mechanism of cell killing. First, we determined the minimal inhibitory concentrations (MICs) for the anti-*acpP* peptide-PNA, a control sequence scrambled version of the anti-*acpP* peptide-PNA and four conventional antibiotics in parallel against *E. coli* (Table 1 and Figure 1). Notably, the MIC for this peptide-PNA was 0.8 μmol/l, making it more potent on a molar basis than ampicillin, chloramphenicol, trimethoprim, and streptomycin (Table 1). Next, we determined the rate of cell killing by equimolar doses of peptide-PNAs and the conventional antibiotics. The results indicate that PNA can rapidly kill *E. coli*, consistent with previous reports,<sup>7,9</sup> although the rate of killing was slower than observed for streptomycin (Figure 1b).

The sequence and gene selectivity of the anti-*acpP* peptide-PNA has been examined and reported.<sup>7,9</sup> To ensure that selectivity was maintained in this study, we included the sequence scrambled version of the peptide-PNA. Again, the control molecule was not inhibitory in the cell kill assay. Also, we determined the effect of the targeted and control peptide-PNAs on *acpP* mRNA abundance in growing cells treated with sub-lethal concentrations using real-time reverse transcriptase-polymerase chain reaction. As expected, the targeted anti-*acpP* peptide-PNA reduced *acpP* mRNA abundance and the scrambled version was not inhibitory (Figure 1c). These results are consistent with mRNA reduction in the presence of antisense PNAs,<sup>17</sup> and the data support a target selective antisense mechanism.

### Peptide-PNA treated bacteria remain intact

Bactericidal effects of antimicrobials may be associated with cell lysis or membrane damage. To test whether peptide-PNA treatment leads to cell lysis, anti-*acpP* peptide-PNA-treated cells were incubated with the nucleic acid ligands SYTOX Green and 4',6-diamidino-2-phenylindole (DAPI) and then observed using

fluorescence microscopy. Both probes stain DNA and RNA and display enhanced fluorescence upon binding. However, the two probes differ in cell entry properties: DAPI freely enters both live and dead cells, whereas SYTOX Green is normally excluded from bacteria; positive green staining is taken as an indication of cell death.<sup>20</sup> PNA-treated cells were compared to untreated and heat-killed bacteria. All cells were stained with DAPI, and both the peptide-PNA- and heat-treated cells were stained with SYTOX Green, indicating that the peptide-PNA-treated cells were non-viable (Figure 1d). The results show that peptide-PNA-killed cells did not lyse but were elongated (Figure 1d). Finally, total nucleic acids were isolated from the untreated and treated cells and peptide-PNA treatment did not appear to alter nucleic acid content (data not shown).

### PNAs accumulate in bacteria

Given that the anti-*acpP* peptide-PNA is bactericidal but does not lyse cells, we considered the possibility that PNAs may accumulate in bacteria or show a long retention period following exposure. To address this question, we used two experimental techniques.

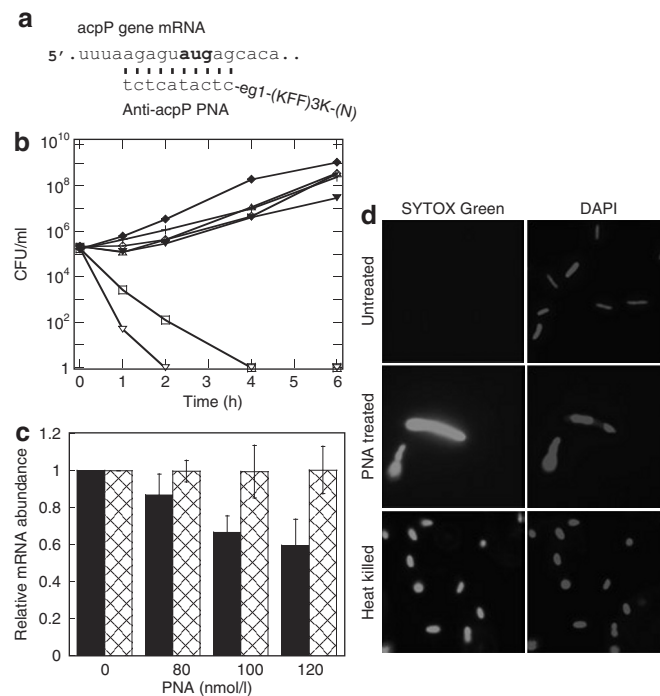


**Figure 1** Bactericidal effects of an anti-acyl carrier protein (anti-*acpP*) peptide-PNA and conventional antibiotics against *Escherichia coli*. (a) The structure of *acpP* messenger RNA (mRNA) and anti-*acpP* peptide-PNA. (b) Cultures of *E. coli* K12 were untreated (♦) or treated with anti-*acpP* peptide-PNA (□), anti-*acpP* peptide-PNA scrambled control (◇), streptomycin (▽), chloramphenicol (+), ampicillin (Δ), and trimethoprim (▼) at 2 μmol/l. Colony forming units (CFUs) were scored by culture dilution and plating. (c) Effect of targeted anti-*acpP* peptide-PNA (solid bars) and anti-*acpP* peptide-PNA scrambled control (hatched bars) treatment on *acpP* mRNA abundance (d) Effect of anti-*acpP* peptide-PNA treatment on cell morphology, nucleic acid content, and cell viability. Control, heat-treated, and anti-*acpP* peptide-PNA-treated cultures of *E. coli* K12 were stained with SYTOX Green and 4',6-diamidino-2-phenylindole (DAPI) and then observed by fluorescence microscopy (×1000). PNA, peptide nucleic acid.

**Table 1** MIC and the duration of PAE of antibacterial agents against *Escherichia coli* K12

Antibacterial	MIC (μmol/l)	PAE duration (h) ± std
Ampicillin	12.5	1.05 ± 0.28
Chloramphenicol	8	2.23 ± 0.36
Streptomycin	1.25	7.32 ± 0.91
Trimethoprim	2	0.89 ± 0.28
Anti <i>acpP</i> peptide-PNA	0.8	11.70 ± 2.6
Anti <i>acpP</i> peptide-PNA scrambled	8	not determined

Abbreviations: *acpP*, acyl carrier protein; MIC, minimal inhibitory concentration; PAE, post-antibiotic effect; PNA, peptide nucleic acid.

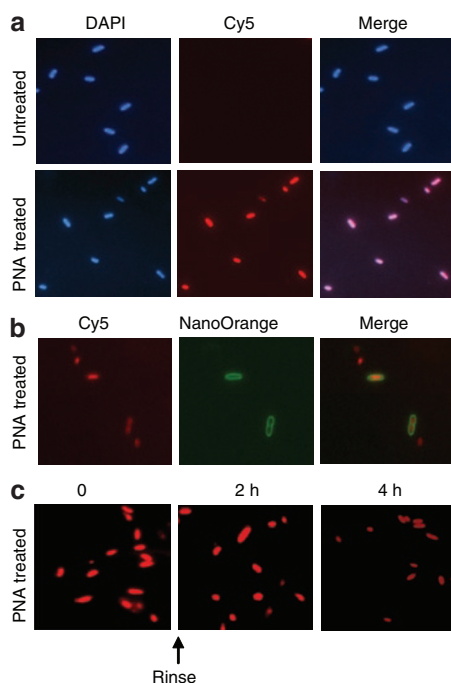


**Figure 2** Accumulation of fluorophore labeled peptide nucleic acid (PNA). *Escherichia coli* was treated with fluorophore labeled peptide-PNA and observed by fluorescence microscopy ( $\times 1000$ ). **(a)** *E. coli* cells were treated with ULS-Cy5 labeled anti-*lacZ* peptide-PNA and counter stained with 4',6-diamidino-2-phenylindole (DAPI). **(b)** *E. coli* cells were treated with ULS-Cy5 labeled anti-*lacZ* peptide-PNA. Cell membranes were counter stained with NanoOrange. **(c)** *E. coli* cells were treated with ULS-Cy5 labeled anti-*lacZ* peptide-PNAs and viewed following a rinse cycle at 2 and 4 hours.

First, to avoid complications associated with cell death caused by the bactericidal peptide-PNA, a non-toxic anti-*lacZ* peptide-PNA was used in the transit experiments. The anti-*lacZ* peptide-PNA was labeled with the universal labeling system (ULS)-Cy5 fluorophore, and we observed the level of cell-associated Cy5 fluorescence in cells that were counter stained with the nucleic acid stain DAPI or the membrane stain NanoOrange. When Cy5 labeled peptide-PNAs were used together with DAPI, the level of cell-associated Cy5 fluorescence was much higher than in the surrounding media, indicating that labeled peptide-PNA accumulated with cells (**Figure 2a**). In this experiment, it is important to note that the cells were not rinsed before microscopy, which allowed us to view cellular accumulation. Also, the quantum yield for cyanine dyes does not alter substantially in different cellular environments, whereas DAPI and NanoOrange fluorescence quantum yield increases greatly when these dyes bind to nucleic acids and proteins, respectively. When the ULS-Cy5 labeled peptide-PNA was used together with NanoOrange, the Cy5 fluorescence appeared to accumulate in cells. Red fluorescence was visible inside the halo of NanoOrange fluorescence, indicating that a proportion of the labeled PNAs were localized in the bacterial cytoplasm (**Figure 2b**). Therefore, although qualitative, the fluorescence data indicate an accumulation of PNA in cells. Finally, to monitor the efflux of fluorophore labeled PNAs, cells were treated as described above, rinsed once with fresh media, and then viewed after 2 and 4 hours. Cell-associated fluorescence was retained but was reduced at 4 hours, indicating a slow rate of efflux (**Figure 2c**).

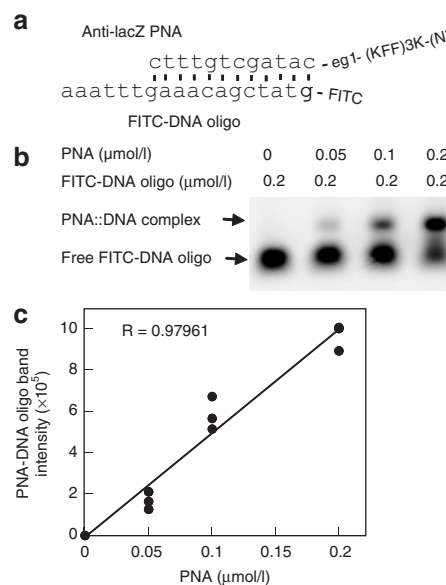


**Figure 3** Quantification of cell-associated peptide nucleic acid (PNA) in cell lysates. Standard curves for PNA in cell lysates. **(a)** The structure of anti-*lacZ* peptide-PNA along with the complementary FITC-DNA oligomer. **(b)** Gel shift analysis of hybridized PNA in a 3% agarose gel. **(c)** PNA::DNA band intensity was plotted against PNA concentration to provide a standard curve. FITC, fluorescein isothiocyanate.

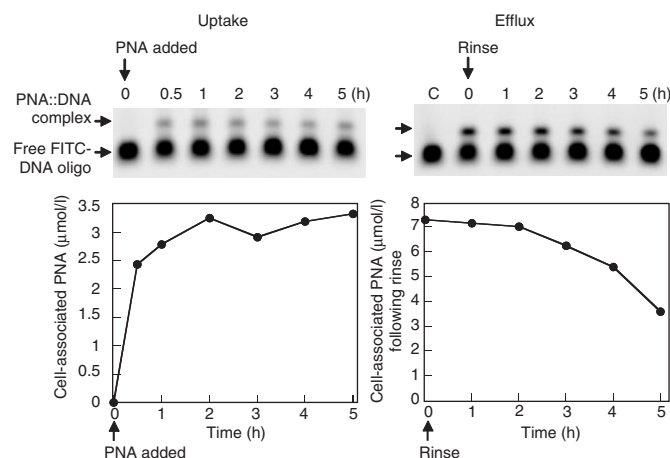


**Figure 4** Uptake and efflux kinetics. The gel shift shows retarded bands, which indicate cell-associated anti-*lacZ* peptide-PNA. A free FITC-DNA oligomer was used as a control (c; lane 1). Cell-associated PNA concentrations were determined using a standard curve and then plotted. FITC, fluorescein isothiocyanate; PNA, peptide nucleic acid.

Second, to assess peptide-PNA uptake and efflux rates using a quantitative method, we established a gel shift assay for cell-associated anti-*lacZ* peptide-PNA as in a method previously used to determine PNA concentration in brain tissue.<sup>21</sup> An advantage with this assay is that it can be applied to unlabeled PNAs. A labeled complementary DNA oligonucleotide is used, and formation of a DNA::PNA duplex is observed as a retarded band following fractionation using agarose gel electrophoresis. To generate a standard curve, *E. coli* cell lysates were spiked with anti-*lacZ* peptide-PNA, allowed to hybridize with fluorescein isothiocyanate (FITC)-labeled complementary DNA oligonucleotides for 3 hours, and then subjected to gel electrophoresis

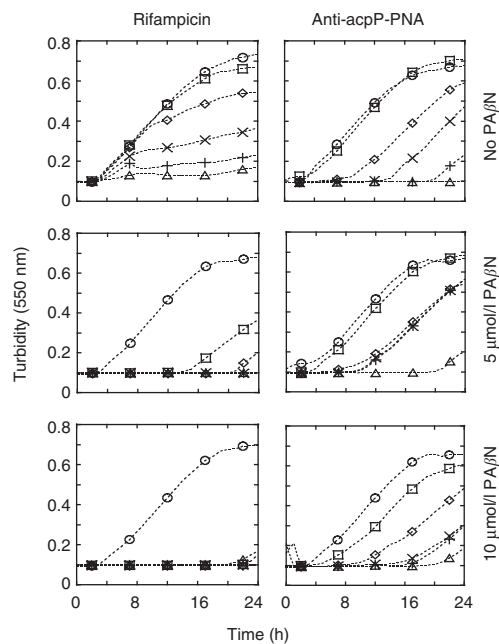


**Figure 5** Growth of *Escherichia coli* K12 treated with rifampicin or anti-*acpP* peptide-PNA in combination with the efflux pump inhibitor Phe-Arg- $\beta$ -naphthylamide (PA $\beta$ N). Growth was measured by monitoring culture turbidity at optical density (OD<sub>550</sub>). The panel at left shows cultures treated with 0 ( $\circ$ ), 2 ( $\square$ ), 4' ( $\diamond$ ), 6 ( $\times$ ), 8 (+), and 10  $\mu$ mol/l ( $\Delta$ ) rifampicin in the absence or presence of PA $\beta$ N (0, 5, 10  $\mu$ mol/l). The panel at right shows growth of cultures treated with 0 ( $\circ$ ), 0.15 ( $\square$ ), 0.3 ( $\diamond$ ), 0.45 ( $\times$ ), 0.6 (+), and 0.75  $\mu$ mol/l ( $\Delta$ ) anti-*acpP* peptide-PNA in the absence or presence of PA $\beta$ N (0, 5, and 10  $\mu$ mol/l). *acpP*, acyl carrier protein; PNA, peptide nucleic acid.

(**Figure 3**). The fluorescent images were collected (**Figure 3b**) and quantified using image analysis software and then plotted (**Figure 3c**). The standard curve was used to quantify cell-associated PNA in the subsequent analyses.

To determine uptake kinetics, freshly grown *E. coli* cultures were treated with 2  $\mu$ mol/l anti-*lacZ* peptide-PNA; samples were harvested at intervals up to 5 hours, rinsed thoroughly, and subjected to PNA quantification (**Figure 4**). The data indicate that the cell-associated PNA concentration exceeded the initial medium concentration (2  $\mu$ mol/l) within 30 minutes. The amount of cell-associated PNA increased further up to 5 hours.

To determine efflux kinetics, *E. coli* were grown in the presence of 2  $\mu$ mol/l anti-*lacZ* peptide-PNA for 20 hours and then rinsed with fresh media; samples were harvested at time intervals up to 5 hours and analyzed as described above. The gel shift profile and the PNA efflux kinetics are illustrated in **Figure 4**. The data indicate that PNA accumulated to 7.3  $\mu$ mol/l in bacteria after 20 hours and was retained at comparatively high concentrations (>3.5  $\mu$ mol/l) for up to 5 hours.

### The efflux pump inhibitor Phe-Arg- $\beta$ -naphthylamide does not affect peptide-PNA potency

Efflux pumps in bacteria reduce the potency of many antimicrobials and provide a common mechanism of multi-drug resistance. The slow efflux kinetics for PNA described here, together with previous results using mutant bacteria,<sup>22</sup> suggest that PNAs are unlikely to be substrates for efflux pumps. To examine this

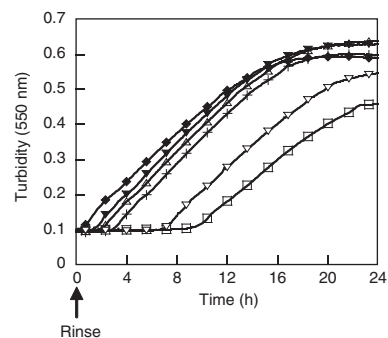


**Figure 6** Post-antibiotic effect (PAE). Cultures of bacteria were untreated ( $\blacklozenge$ ) or treated for 1 hour with anti-*acpP* peptide-PNA ( $\square$ ), streptomycin ( $\nabla$ ), chloramphenicol (+), ampicillin ( $\Delta$ ), and trimethoprim ( $\blacktriangledown$ ) at  $\times 5$  their MIC. The PAEs are shown as representative curves from five replicate experiments (see **Table 1**). MIC, minimal inhibitory concentration.

issue further, we used the efflux pump inhibitor Phe-Arg- $\beta$ -naphthylamide (PA $\beta$ N), which inhibits a broad spectrum of efflux pumps in a variety of gram-negative bacteria and also dramatically sensitizes *E. coli* to several antibiotics.<sup>23</sup> *E. coli* were treated with increasing doses of PA $\beta$ N and also with increasing doses of rifampicin or anti-*acpP* peptide-PNA. The effects on growth are illustrated in **Figure 5**. Whereas the inhibitory concentrations for rifampicin were dramatically reduced by PA $\beta$ N, peptide-PNA activity was unchanged. Therefore, the results using this pump inhibitor support the notion that antisense antibacterials are unlikely substrates for efflux pumps.

### Anti-*acpP* peptide-PNAs display a long PAE

To determine whether the accumulation and retention of PNA in *E. coli* results in a long PAE, we subjected peptide-PNA and four conventional antibiotics to a standard PAE assay.<sup>24</sup> *E. coli* growth was severely delayed in the presence of streptomycin and anti-*acpP* peptide-PNA relative to the other antibiotics tested (**Figure 6**; **Table 1**).

## DISCUSSION

The results of this study show that the anti-*acpP* peptide-PNA is more potent than several conventional antimicrobials in standard MIC and cell killing assays. Also, peptide-PNA treatment did not lyse cells or alter gross cellular integrity or content. The bactericidal activity of conventional antimicrobials is often associated with cell lysis; therefore, it is important to understand the mechanisms that underlie the activity of antisense antibacterials. If it is true that antisense peptide-PNAs kill cells in the absence of lysis, then cell killing is likely to involve a long period of PNA retention. The anti-*acpP* peptide-PNA targets an essential fatty acid biosynthesis gene, and cells that retain PNA may be unable to divide and may die from a lack of fatty acid biosynthesis even after the growth environment has been depleted of PNA. PNA retention could involve target affinity, carrier peptide decay, or an inability to exit across asymmetric cell membrane structures and charge gradients.

The results from fluorescence microscopy of labeled PNAs and quantification of cell-associated unlabeled PNAs indicate rapid uptake, slow efflux, and an accumulation in cells. The results for cell retention are striking: the literature indicates that

conventional antibiotics efflux from *E. coli* within minutes,<sup>25</sup> whereas PNAs are retained for several hours (Figures 2 and 4). Also, PNAs do not appear to be removed by efflux pumps. A long period of cellular retention suggested that these molecules would display a long PAE. Indeed, we observed a PAE of >11 hours (Table 1), which to our knowledge is longer than other examples reported in the literature. Therefore, PNAs accumulate in bacteria, are retained without active efflux, and show a long PAE. These properties appear to explain the potent bactericidal effects observed *in vitro* and *in vivo*.<sup>9,11,13</sup>

A criticism against efforts to develop antisense oligomers as drugs, and as antimicrobials in particular, is that such molecules are inherently too large to achieve efficient cell uptake and *in vivo* distribution. However, as we have described here, peptide-PNA and peptide-phosphorodiamidate morpholino oligomer based antimicrobials perform well in cell kill assays *in vitro* and *in vivo*. Also, there is renewed interest from clinicians in the efficacy of larger molecular weight antimicrobials.<sup>26</sup> Therefore, mechanisms that explain the activity of relatively large molecular weight antimicrobials should be considered because they may broaden the scope for chemists to develop new classes of antimicrobials.

The present data indicate that the cellular transit kinetics of PNA leads to an accumulation in cells. The delivery of antisense agents into bacteria remains a significant challenge; once delivered, however, the molecule is retained, and this may contribute to potent antimicrobial activity and a long PAE. The antisense mechanism and accumulation propensities may prove particularly appropriate in new strategies for treating persistent, dormant, or drug resistant infections.

## MATERIALS AND METHODS

**Bacteria, growth medium, and antimicrobials.** *E. coli* K12 was obtained from the Coli Genetic Stock Center (<http://cgsc.biology.yale.edu>). Mueller-Hinton (MH) broth, antimicrobial drugs, and PAβN were purchased from Sigma-Aldrich (St. Louis, MO). Cells were grown in 96-well low attachment plates (COSTAR 3474, Corning, Lowell, MA). The anti-*acpP* ((KFF)3K-eg1-ctcactactct), the anti-*acpP* scrambled control ((KFF)3K-eg1-ctcactatctc), and the anti-*lacZ* ((KFF)3K-eg1-catagctgtttc) peptide-PNAs complementary to the start codon regions of the *acpP* and *lacZ* genes, respectively, have been described.<sup>7</sup> The peptide-PNAs were obtained from Panagene (Daejeon, Korea).

**MIC and colony forming unit determinations.** *E. coli* K12 cultures were grown overnight and diluted to  $5 \times 10^5$  cells/ml in MH broth, and 80  $\mu$ l aliquots were added to wells of a low attachment 96-well plate. Antimicrobial aliquots (20  $\mu$ l) of different concentrations were added to give a final volume of 100  $\mu$ l. Plates were incubated for 20 hours at 37°C in a VersaMax spectrophotometer with shaking, and optical density (OD<sub>550</sub>) measurements were taken every 5 minutes. MICs were scored as the lowest concentration of an antimicrobial needed to prevent measurable growth after 20 hours.

To measure colony forming units, antimicrobials were added to bacterial cultures to a final concentration of 2  $\mu$ mol/l, as described previously. Cultures were harvested at 0, 1, 2, 4, and 6 hours. The content of each well was added to 0.9 ml of MH broth and centrifuged at 9300g for 5 minutes. Supernatants were removed and the cell pellets were suspended in fresh pre-warmed MH broth (100  $\mu$ l). Tenfold serial dilutions were prepared, and 20  $\mu$ l aliquots were plated on Luria-Bertani agar plates and incubated overnight at 37°C.

**Relative quantitative polymerase chain reaction of *acpP* mRNA in peptide-PNA-treated *E. coli*.** *E. coli* K12 cultures were grown overnight

and diluted to  $5 \times 10^5$  cells/ml in MH broth, and 180  $\mu$ l aliquots were added to the wells of a low attachment 96-well plate. Anti-*acpP* or anti-*acpP* scrambled control peptide-PNAs (20  $\mu$ l) of varying concentrations (0, 80, 100, 120 nmol/l) were added to give a final volume of 200  $\mu$ l. These concentrations were chosen to provide sufficient growth inhibition and RNA yield. The plate was incubated at 37°C in a VersaMax spectrophotometer with shaking, and OD<sub>550</sub> measurements were taken every 5 minutes until an increase in OD<sub>550</sub> of ~0.1 in the untreated cultures was reached. The content of 4–32 wells were pooled for total RNA extraction and treatment with DNase I using the RiboPure Bacteria kit (Ambion (Europe) LTD, Cambridgeshire, UK), according to the manufacturer's protocol. RNA (250 ng) was converted to complementary DNA in a 25  $\mu$ l reaction consisting of 1 $\times$  reverse transcription reaction buffer, 5.5 mmol/l Mg<sup>2+</sup>, 500  $\mu$ mol/l of each dNTP, 2.5  $\mu$ mol/l random hexamers, 10 U RNase inhibitor, and 31.5 U Multiscribe reverse transcriptase (Applied Biosystems, Foster City, CA). Relative quantitative polymerase chain reaction was then carried out with 5 ng of complementary DNA in a 25  $\mu$ l reaction consisting of 1 $\times$  SYBR Green 1 reaction buffer (Eurogentec SA, Seraing, Belgium), 100 nmol/l of *acpP*-F (5'-CAGGAAGAAGTTACCAA CAATGCTT 3') and *acpP*-R (5'-CCAGCTCAACGGTGTCAAGA-3') primers or 100 nmol/l of *rpoA*-F (5'-AAGCTGGTCATCGAAATGGAA-3') and 150 nmol/l of *rpoA*-R (5'-GCCGCACGACGAATCG-3') primers. Amplification efficiencies of the target gene, *acpP*, and the reference gene, *rpoA*, were validated (109%), and data analyses were carried out by the 2<sup>- $\Delta\Delta$ CT</sup> method.<sup>27</sup> The averages of three sample replicates were used to calculate mRNA abundance of peptide-PNA-treated samples relative to untreated samples. The experimental procedure was repeated three times, and mean values with error bars representing standard deviation were plotted as a histogram.

**Fluorescence microscopy.** Freshly grown cells were observed without fixation or post stain rinsing with a Leica DMRA2 microscope (Leica Mikroskopie und Systeme GmbH, Wetzlar, Germany) at  $\times 1000$  and the images were processed using Openlab software version 3.1.4 (Improvision, Coventry, England). To examine cell viability, cells were stained with 1  $\mu$ mol/l SYTOX Green membrane integrity indicator stain (Invitrogen Ltd, Paisley, UK) and DAPI (2  $\mu$ g/ml). To observe peptide-PNA uptake, peptide-PNAs were labeled with Cy5 using the Kreatech ULS (Kreatech Biotechnology, Amsterdam, The Netherlands). In a 500  $\mu$ l microcentrifuge tube, 2  $\mu$ g anti-*lacZ* peptide-PNA was mixed with 2  $\mu$ l reaction buffer, 2  $\mu$ l Cy5-ULS reagent, and water to 20  $\mu$ l total and then incubated at 85°C for 4 hours. The labeled peptide-PNA was purified using a Pierce PepClean C18 spin column (Pierce #89870; Pierce Biotechnology, Rockford, IL). The column was pre-rinsed with 150  $\mu$ l 50% acetonitrile and equilibrated twice with 150  $\mu$ l solution of 5% acetonitrile containing 0.5% trifluoroacetate. The reaction mixture was diluted in 150  $\mu$ l 5% acetonitrile containing 0.5% trifluoroacetate and then loaded onto the column and centrifuged at 1000g. The column was rinsed with a gradient of 10, 20, 25, and 30% acetonitrile (150  $\mu$ l, 0.5% trifluoroacetate). The labeled product was eluted with 70% acetonitrile (0.5% trifluoroacetate), dried under vacuum, and then dissolved in 20  $\mu$ l water. The labeled peptide-PNA was added to cells at 2  $\mu$ mol/l, and the cells were counter stained with a 1/20 dilution of NanoOrange dye (Invitrogen Ltd, Paisley, UK) and DAPI.

**Quantification of cell-associated PNA.** Overnight cultures were diluted to  $5 \times 10^5$  colony forming units/ml in MH broth, and 80  $\mu$ l aliquots were added to the wells of a low attachment 96-well plate. Water or peptide-PNA solution (2  $\mu$ mol/l final) was added to 100  $\mu$ l and the plate was incubated for 24 hours as described above. The contents of two wells were pooled and added to 1.3 ml pre-warmed MH broth in coated 1.5 ml tubes (Maxym Recovery; Axygen Scientific, Union City, CA). Bacteria were harvested by centrifugation for 3 minutes at 2300g. After removing the supernatant, the tubes were briefly centrifuged to remove residual liquid. Cell pellets were resuspended in 1.5 ml pre-warmed MH

broth. The rinse and centrifugation steps were repeated. Cell pellets were resuspended in 5  $\mu$ l water and transferred to a fresh tube. To lyse cells, 15  $\mu$ l yeast protein extraction reagent (Pierce Biotechnology) was added, cells were shaken overnight at room temperature and then sonicated for 10 minutes using 30-second pulses at high intensity in a Diagenode Bioruptor (Diagenode SA, Liege, Belgium). Cell debris was precipitated by 5 minutes of centrifugation at 9300g, and supernatants were transferred to fresh tubes. An FITC-labeled DNA oligonucleotide (5'-aaattgaaacagctatg-3') (Thermo Fisher Scientific, Waltham, MA) was added to 10  $\mu$ l of cell lysate to give 0.2  $\mu$ mol/l in 11  $\mu$ l final volume. The mixture was incubated at 37°C for 3 hours and fractionated by electrophoresis in a 3% agarose gel. The gel was scanned using a Typhoon 9400 Scanner (Amersham Biosciences, Piscataway, NJ) using green excitation (532 nm) and emission (526 nm, short pass) filters and the photomultiplier tube set at 550 V. Images were processed using ImageQuant software version 5 (Amersham Biosciences). To determine the concentration of cell-associated PNA, the concentrations of PNA in cell lysates were related to cell volumes. To estimate cell volumes, cell mass was first determined by drying equivalent aliquots overnight in a Speed-Vac followed by dry weight measurements using an analytical balance. The cell dry weight was taken as  $3.0 \times 10^{-13}$  g/cell and was converted to volume using the value  $1 \times 10^{-15}$  L/cell.

**PAE.** PAE values were determined essentially as described.<sup>24</sup> Cultures of *E. coli* K12 were grown to early exponential phase ( $10^9$  cells/ml) in MH broth in a VersaMax spectrophotometer with shaking. OD<sub>550</sub> measurements were taken at 5-minute intervals. The bacterial cultures were diluted to  $10^7$  cells/ml in MH broth, and 80  $\mu$ l aliquots were added to the wells of a low attachment 96-well plate. Test antimicrobial aliquots (20  $\mu$ l) were added to give  $5 \times$  MIC (100  $\mu$ l final volumes). The 96-well plate was incubated for 60 minutes at 37°C as described above. Bacteria were harvested by centrifugation at 2300g for 5 minutes, and the cell pellets were suspended in fresh pre-warmed MH broth (100  $\mu$ l). The rinse cycle was repeated twice, and the plates were incubated for 24 hours at 37°C as described previously. PAE duration was calculated by subtracting the time taken for the control culture to reach 50% of the OD<sub>max</sub> from the time taken for antimicrobial-treated cultures to reach the same OD.

## ACKNOWLEDGMENTS

We thank the Swedish Research Council, Zabol University, and the Iranian Ministry of Science for support. E. J. K. is an employee of KREATECH Biotechnology B.V.

## REFERENCES

- Keren, I, Shah, D, Spoering, A, Kaldalu, N and Lewis, K (2004). Specialized persister cells and the mechanism of multidrug tolerance in *Escherichia coli*. *J Bacteriol* **186**: 8172–8180.
- Wagner, EG, Altuvia, S and Romby, P (2002). Antisense RNAs in bacteria and their genetic elements. *Adv Genet* **46**: 361–398.
- Nielsen, PE, Egholm, M, Berg, RH and Buchardt, O (1991). Sequence-selective recognition of DNA by strand displacement with a thymine-substituted polyamide. *Science* **254**: 1497–1500.
- Stirchak, EP, Summerton, JE and Weller, DD (1989). Uncharged stereoregular nucleic acid analogs: 2. Morpholino nucleoside oligomers with carbamate internucleoside linkages. *Nucleic Acids Res* **17**: 6129–6141.
- Lehtola, MJ, Loades, CJ and Keevil, CW (2005). Advantages of peptide nucleic acid oligonucleotides for sensitive site directed 16S rRNA fluorescence *in situ* hybridization (FISH) detection of *Campylobacter jejuni*, *Campylobacter coli* and *Campylobacter lari*. *J Microbiol Methods* **62**: 211–219.
- Prescott, AM and Fricker, CR (1999). Use of PNA oligonucleotides for the *in situ* detection of *Escherichia coli* in water. *Mol Cell Probes* **13**: 261–268.
- Good, L, Awasthi, SK, Dryselius, R, Larsson, O and Nielsen, PE (2001). Bactericidal antisense effects of peptide-PNA conjugates. *Nat Biotechnol* **19**: 360–364.
- Eriksson, M, Nielsen, PE and Good, L (2002). Cell permeabilization and uptake of antisense peptide-peptide nucleic acid (PNA) into *Escherichia coli*. *J Biol Chem* **277**: 7144–7147.
- Tan, XX, Actor, JK and Chen, Y (2005). Peptide nucleic acid antisense oligomer as a therapeutic strategy against bacterial infection: proof of principle using mouse intraperitoneal infection. *Antimicrob Agents Chemother* **49**: 3203–3207.
- Faridani, OR, Nikravesh, A, Pandey, DP, Gerdes, K and Good, L (2006). Competitive inhibition of natural antisense Sok-RNA interactions activates Hok-mediated cell killing in *Escherichia coli*. *Nucleic Acids Res* **34**: 5915–5922.
- Geller, BL, Deere, J, Tilley, L and Iversen, PL (2005). Antisense phosphorodiamidate morpholino oligomer inhibits viability of *Escherichia coli* in pure culture and in mouse peritonitis. *J Antimicrob Chemother* **55**: 983–988.
- Geller, BL, Deere, JD, Stein, DA, Kroeker, AD, Moulton, HM and Iversen, PL (2003). Inhibition of gene expression in *Escherichia coli* by antisense phosphorodiamidate morpholino oligomers. *Antimicrob Agents Chemother* **47**: 3233–3239.
- Tilley, LD, Mellbye, BL, Puckett, SE, Iversen, PL and Geller, BL (2007). Antisense peptide-phosphorodiamidate morpholino oligomer conjugate: dose-response in mice infected with *Escherichia coli*. *J Antimicrob Chemother* **59**: 66–73.
- Gruegelsiepe, H, Brandt, O and Hartmann, RK (2006). Antisense inhibition of RNase P: mechanistic aspects and application to live bacteria. *J Biol Chem* **281**: 30613–30620.
- Nekhotiaeva, N, Awasthi, SK, Nielsen, PE and Good, L (2004). Inhibition of *Staphylococcus aureus* gene expression and growth using antisense peptide nucleic acids. *Mol Ther* **10**: 652–659.
- Kurupati, P, Tan, KS, Kumarasinghe, G and Poh, CL (2007). Inhibition of gene expression and growth by antisense peptide nucleic acids in a multidrug-resistant  $\beta$ -lactamase-producing *Klebsiella pneumoniae*. *Antimicrob Agents Chemother* **51**: 805–811.
- Dryselius, R, Nikravesh, A, Kulyte, A, Goh, S and Good, L (2006). Variable coordination of cotranscribed genes in *Escherichia coli* following antisense repression. *BMC Microbiol* **6**: 97.
- Kulyte, A, Nekhotiaeva, N, Awasthi, SK and Good, L (2005). Inhibition of *Mycobacterium smegmatis* gene expression and growth using antisense peptide nucleic acids. *J Mol Microbiol Biotechnol* **9**: 101–109.
- Williams, KJ and Piddock, LJ (1998). Accumulation of rifampicin by *Escherichia coli* and *Staphylococcus aureus*. *J Antimicrob Chemother* **42**: 597–603.
- Lebaron, P, Catala, P and Parthuisot, N (1998). Effectiveness of SYTOX Green stain for bacterial viability assessment. *Appl Environ Microbiol* **64**: 2697–2700.
- McMahon, BM, Mays, D, Lipsky, J, Stewart, JA, Fauq, A and Richelson, E (2002). Pharmacokinetics and tissue distribution of a peptide nucleic acid after intravenous administration. *Antisense Nucleic Acid Drug Dev* **12**: 65–70.
- Good, L, Sandberg, R, Larsson, O, Nielsen, PE and Wahlestedt, C (2000). Antisense PNA effects in *Escherichia coli* are limited by the outer-membrane LPS layer. *Microbiology* **146**: 2665–2670.
- Saenz, Y, Ruiz, J, Zarazaga, M, Teixido, M, Torres, C and Vila, J (2004). Effect of the efflux pump inhibitor Phe-Arg-beta-naphthylamide on the MIC values of the quinolones, tetracycline and chloramphenicol, in *Escherichia coli* isolates of different origin. *J Antimicrob Chemother* **53**: 544–545.
- Stubbings, WJ, Bostock, JM, Ingham, E and Chopra, I (2004). Assessment of a microplate method for determining the post-antibiotic effect in *Staphylococcus aureus* and *Escherichia coli*. *J Antimicrob Chemother* **54**: 139–143.
- George, AM and Hall, RM (2002). Efflux of chloramphenicol by the CmlA1 protein. *FEMS Microbiol Lett* **209**: 209–213.
- Falagas, ME and Michalopoulos, A (2006). Polymyxins: old antibiotics are back. *Lancet* **367**: 633–634.
- Livak, KJ and Schmittgen, TD (2001). Analysis of relative gene expression data using real-time quantitative PCR and the 2(-Delta Delta C(T)) method. *Methods* **25**: 402–408.